Available online at www.sciencedirect.com
ScienceDirect
Soils and Foundations 65 (2025) 101631
www.elsevier.com/locate/sandf

Technical Paper

Drilling parameters as predictors of the measured full scale performance of CFA piles by using statistical analysis of CPT profiles: a case study

Gianpiero Russo [a], Ilaria Esposito [a], Massimo Ramondini [a], Alessia Vecchietti [b], Giacomo Russo [c]

[a] *Department of Civil and Environmental Engineering, University of Napoli Federico II, Italy*
[b] *Pizzi Instruments, Firenze, Italy*
[c] *Department of Earth Sciences, Environment and Resources, University of Napoli Federico II, Italy*

Received 24 December 2024; received in revised form 7 May 2025; accepted 18 May 2025
Available online 30 May 2025

Abstract

The Continuous Flight Auger (CFA) piles, also known as Auger Cast In Place piles (ACIP), have a widespread use in the world market of replacement concrete piles. The installation of such piles is generally made by equipment which records several significant installation parameters, as the torque M_t and the axial force N, applied during the auger advancing step. In the auger retrieval stage other parameters that can influence the load-settlement performance of the pile are monitored. The paper presents a case study dealing with the CFA piles adopted as a foundation for a water treatment basin. In the paper first the equations governing the kinematical analysis of the augering and concreting stages of the pile construction are introduced. After the description of the test site with the subsoil conditions and the presentation of a typical sets of parameters recorded during pile installation the results of two pile loading tests to failure are reported. A new approach for determining the depth of the soil layers boundaries, based on the statistical analysis of CPT profiles with depth, is proposed and successfully applied confirming the qualitative geological analysis of the site. A further statistical analysis is carried out to find a robust correlation between the q_c of the CPT and the torque M_t needed to screw in depth the auger for pile construction. Finally, virtual CPT profiles generated from the torque M_t recorded during the tested piles installation are used for piles bearing capacity calculations which are compared with the results of pile loading tests. The successful comparison reported in the paper is a first step to validate the proposal to use parameters recorded during augering to calculate and/or to confirm design values of the bearing capacity.

Keywords: CFA piles; Augering process; Installation parameters; CPT profiles; Spatial variability; Statistical analysis; Loading test; Bearing capacity

1. Introduction

Continuous Flight Auger (CFA) piles, also known as Auger Cast In Place piles (ACIP), have a widespread use and occupy a significant portion of the replacement concrete piles' global market. They are rather versatile piles but with the additional advantage of not requiring the support of the hole wall (Van Weele, 1988; Van Impe & Peiffer, 1997; Brown et al., 2007). The construction of a CFA pile is divided into the following stages: positioning of the drilling rig, drilling, concrete pouring and extraction of the propeller and insertion of the reinforcement cage. Drilling is

E-mail address: ilaria.esposito3@unina.it (I. Esposito)

https://doi.org/10.1016/j.sandf.2025.101631
0038-0806/

carried out by advancing into the ground, under the simultaneous action of an axial force and a torque, a helical auger with a hollow central rod closed at the bottom by a disposable drill bit. Penetration into the soil takes place usually without significant removal of the latter. As the auger advances, attention is paid to the relationship between the penetration rate and the rotational speed of the tool. If the auger rotates too quickly compared to the degree of penetration into the ground, transport of soil to the surface due to the *cochlea* effect may occur. As a result, the lateral movement of the soil towards the hole may reduce the confinement around the piles already installed nearby. During the augering step the ratio between the rate of penetration and the rate of revolution of the auger is generally kept at values less than the pitch of the screw. The penetration thus involves both lateral compression and soil extraction. Further removal of soil occurs of course during the auger extraction stage when the casting begins by pumping pressurized concrete through the central hollow stem. When the pile shaft is formed by concreting, the reinforcement cage is inserted into the fresh concrete. At the end of the process if the volume of the removed soil is less than the final volume of the pile, a net compression effect on the soil surrounding the pile is expected; the resulting stress state within the soil is somewhat intermediate between that of a replacement pile and that of a displacement one. A few quantitative data about above details maybe useful. The engines on the piling machines apply a torque action in the range 90–400 kNm. The external diameter of the auger (i.e. the outer nominal diameter of the pile) is in the range 350–900 mm while the external diameter of the central stem is in the range 140–160 mm. Of course, the performance of the pile is affected by all the above constructional details both in terms of stiffness and of bearing capacity. At the design stage the bearing capacity of CFA piles is predicted by semi-empirical methods mostly based on CPT results (Eslami and Fellenius, 1997; Han et al., 2017; Niazi and Mayne, 2016; Xu and Lehane, 2008; Viggiani, 1993; Chen et al., 2020; Heidarie Golafzani et al., 2020; Dohan & Lehane, 2021; Leetsaar et al., 2023). In the following, a case study of a main water basin on a large piled foundations with over 1000 CFA piles is presented. The subsoil, a loose to medium silty sand, was investigated via CPT profiles and two pilot load tests on CFA instrumented piles were carried out at the design stage. Installation parameters applied by the piling rig were carefully recorded for a subgroup of the piles of the basin and for the two piles load tested. A new methodology based on statistical analysis is described and applied to the following problems: a more objective determination of the soil layering using CPT profiles and the prediction of the bearing capacity of the two tested piles by using CPT method applied on synthetic CPTs generated by drilling parameters recorded during their executions. The satisfactory comparison between the calculated and the measured bearing capacities is finally discussed.

2. Kinematical analysis of the augering and concreting processes

The balance between the advancement vertical speed and the rotational velocity of the auger can be converted into equations that govern the kinematical process of the soil augering (Viggiani, 1993). During drilling, the auger with its central stem advances by means of an intermediate mechanism between the advancement of a screw and that of a *cochlea*. Being v the vertical velocity of the auger, d_0 the diameter of the central stem and d the diameter of the auger envelope, n the rotational speed and l the pitch of the screw (Fig. 1), during the time interval Δt the volume of the displaced soil is:

$$V_d = \frac{\pi}{4} d_0^2 v \Delta t \tag{1}$$

while in the same interval the volume of removed soil by *cochlea* effect is:

$$V_a = \frac{\pi}{4}\left(d^2 - d_0^2\right)(nl - v)\Delta t \tag{2}$$

If $v = nl$, the volume of the removed soil is nihil; the auger advances in the soil without any soil removal. If $v = 0$, the auger rotates without any advancement working as a perfect Archimedean *cochlea* and the soil is continuously removed. As intermediate and most common situation the net effect of an overall compression on the soil is obtained if $V_d \geq V_a$, thus resulting in:

$$v \geq nl\left(1 - \frac{d_0^2}{d^2}\right) = v_{crit} \tag{3}$$

The right side of the Eq. (3) is called critical velocity v_{crit} and it has a rather obvious physical meaning.

If $v > v_{crit}$, the volume of displaced soil is larger than the volume of removed soil with a consequent net compression effect; if $v < v_{crit}$, the reverse is true, and the effect is soil

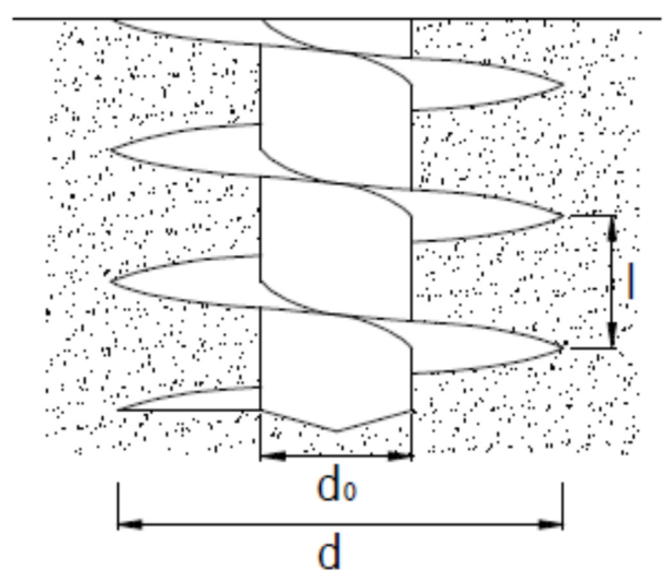

Fig. 1. Auger section.

loosening with a consequent worsening of the expected pile performance.

To have sufficient vertical velocity, at the beginning of the augering process (i.e. down to a depth of 4–6 d) the piling machine needs both a sufficient weight and a hydraulic jack with an adequate axial capacity. If this is not verified the condition $v < v_{crit}$ occurs and the auger acts as an Archimedean *cochlea*; as a consequence the soil surrounding the auger is loosened and after a while the penetration rate increases. In such a case the pile performance will be worse than in the case $v > v_{crit}$.

Once the desired depth is reached, the casting begins by pumping pressurized concrete through the central hollow rod while raising the auger. In this phase, the soil between the coils of the auger is removed. In this stage the ascent rate v_R (i.e. the speed at which the auger is recovered) in relation to the flow of concrete plays an important role and governs the actual geometry of the pile.

During the ascent step, the concrete is pumped through the hollow stalk at the prescribed rate Qc. In the time interval Δt, the volume of poured concrete V_c is equal to:

$$V_c = Q_c * \Delta t \tag{4}$$

while the upward displacement of the auger, Δ, is:

$$\Delta = v_R * \Delta t \tag{5}$$

The average cross-section A_{av} and, thus, the mean diameter d_{av} of the pile over the length Δ can be expressed as:

$$A_{av} = \frac{V_c}{\Delta} = \frac{Q_c}{v_R} \tag{6}$$

$$d_{av} = \sqrt{\frac{4 * A_{av}}{\pi}} = \sqrt{\frac{4 * Q_c}{\pi * v_R}} = 1.13 * \left(\frac{Q_c}{v_R}\right)^{0,5} \tag{7}$$

As shown by (7) a smaller diameter can be provided by either a high retrieval velocity v_R or a small concrete rate Q_c. Of course, the reverse is interesting too and a larger diameter (Mandolini et al., 2002) can be obtained by managing the same ratio.

As noted by Van Impe e Peiffer (1997), Van Weele (1988), Massarsch et al. (1988), Viggiani (1993), Zelada & Stephenson (2000), Mandolini et al. (2002), Russo & Mandolini (2003), Brown et al. (2007), Dohan & Lehane (2021), during both the drilling phase and the subsequent retrieval step several parameters, relatable to the expected pile performance, are potentially recorded.

3. Geotechnical investigations and subsoil conditions at the test site

The test site is located in the plain of the Sarno river close to the Vesuvius volcano. The area occupied by the plant is 150 m × 400 m (Fig. 2). As shown in Fig. 2, the Water Treatment Basin, the largest rectangular tank founded on a 0.9 m thick reinforced concrete piled raft consisting of 1009 CFA settlement reducing piles (d = 800 mm and L = 27 m) is located in the central area of the plant.

In the whole area, characterized by a relatively uniform soil layering, 5 boreholes (depth 24 m ~ 51 m) with undisturbed/disturbed samples for laboratory tests have been carried out (Fig. 2). Two main lithotypes characterize the site (Fig. 3): a lacustrine/alluvial soil constituted by pyroclastic sand and silt (AL) with an average but rather variable thickness of 16 m ~ 20 m, above the ignimbrite campana formation (De Maio et al., 2014), made of slightly cemented pozzolana (silty sands) and grey tuff levels (TG), that extends down to 50 m.

Site investigations consisted of CPTs, CPTUs and SCPTUs (18CPTs + 8CPTUs + 3 SCPTUs). All these tests were carried out with the same probe velocity which is about 20 mm/s as required by international standards (ASTM D5778) and is widely accepted that the tip resistance qc is not dependent on the type of used device. The measured tip resistance q_c (Fig. 4) in the shallower sandy silt layer ranges in the field 2 MPa ~ 4 MPa. In the sublayers, where the sand is slightly prevailing, the q_c ranges in the field 4 MPa ~ 7 MPa, while for the underlying ignimbrite formation (TG) the value of q_c gets up to 20 MPa ~ 25 MPa. A careful scan of the data in Fig. 4 reduces the only significant source of variability of the profiles to the passage from the above alluvial layer (AL) to the below pyroclastic formation (TG).

The average physical and mechanical properties of the two layers based on these results and on those obtained from laboratory tests are summarized in Table 1.

4. Drilling parameters

For the purpose of this study, a subgroup of 45 CFA piles (Fig. 5) selected from the 1009 piles in the foundation of the WTB have been considered. For this subgroup a detailed monitoring of all the drilling parameters was actuated.

The drilling machines were equipped with Jean-Lutz recording system that allowed for continuous monitoring and storage of drilling parameters. The central stem of the auger had an external diameter of 0.160 m while the pitch l of the auger was 0.80 m. During the drilling penetration phase rotation velocity n (rpm), penetration velocity v and torque M_t with depth, were recorded. During the helix extraction, concrete volume Q_c and pressure, and retrieval velocity v_R with depth were further recorded.

It has been long recognized that the torque is closely related to the mechanical shear strength of the soil. For such reason and according to several authors (Gouvenot et al.,1990; Bustamante, 2003) it is not at all surprising that the torque trends may follow very closely CPT profiles. To better understand such a finding, it should be kept in mind that because of the simple relationships illustrated in section 2 dedicated to kinematical analysis of the augering process, there is an increasing awareness among piling operators of the importance of keeping drilling velocity above the critical value v_{crit} provided by Eq. (3). It comes out that the applied torque is typically adjusted during dril-

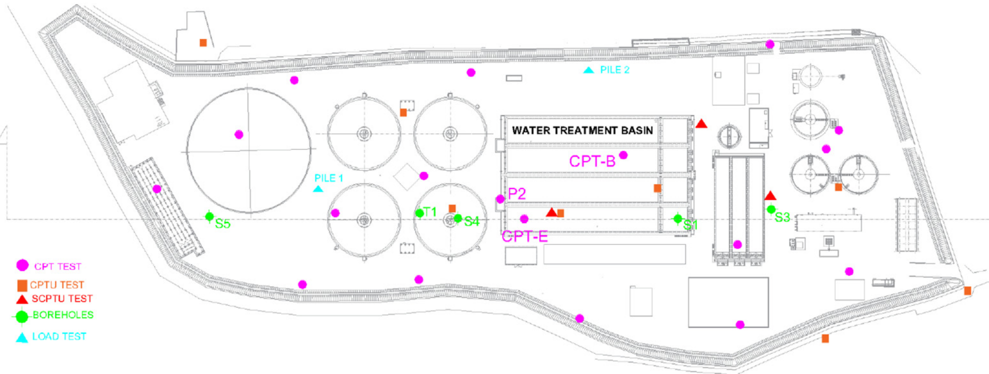

Fig. 2. Sewage treatment plant – Plan view and site investigations.

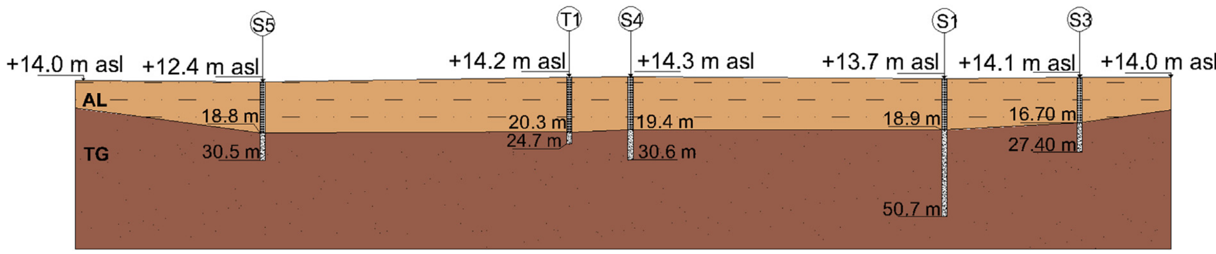

Fig. 3. Section 1-1 of the test site, with ground level (in meters above sea level – m asl) and the depth of the two main soil layers according to the boreholes.

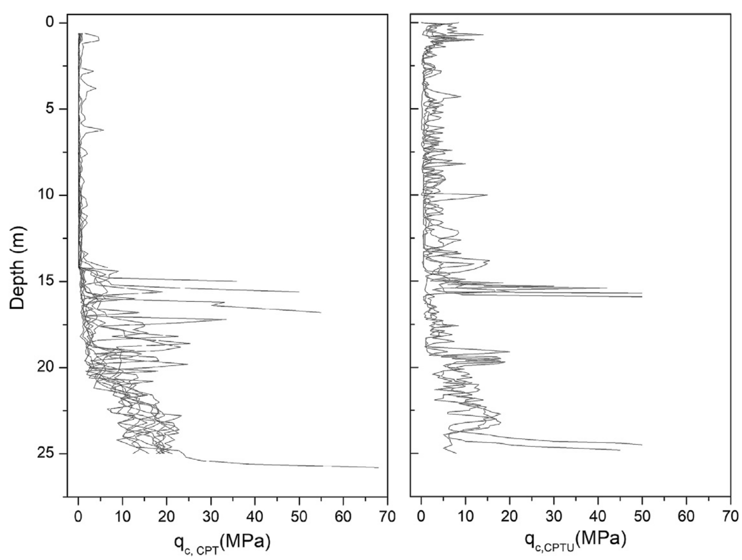

Fig. 4. Cone resistance q_c measured with CPT (left) and with CPTU/SCPTU profiles (right).

Table 1
Physical and Mechanical properties of the soil layers. γ =unit weight, ϕ'= effective stress friction angle, c'= effective cohesion, E_d = oedometer modulus, v_s = shear wave velocity and G_0 = shear modulus at low strain obtained by site geophysical tests (SCPTU).

	Depth (m)	γ (kN/m^3)	ϕ' (°)	c' (kPa)	E_d (MPa)	v_s (m/s)	G_0 (MPa)
Alluvial soil AL	0.00 ~ 17.00	15.8	28 ~ 32	0	0.5 ~ 5	70 ~ 150	8 ~ 32
Ignimbrite TG	17.00 ~ 50.00	15.6	35	–	20	170 ~ 450	45 ~ 300

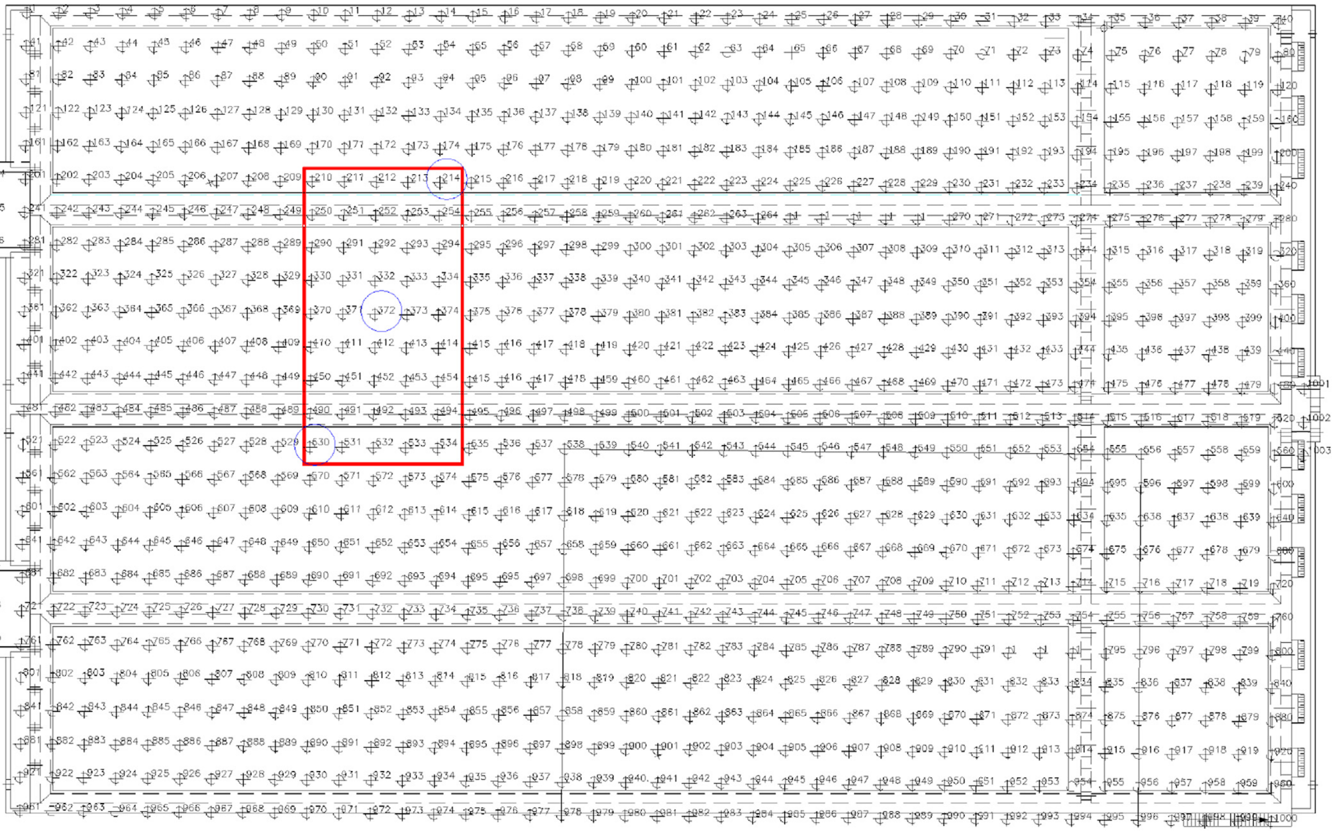

Fig. 5. Water Treatment Basin plan view with 45 CFA pile subgroup analysed for the study (red box) and piles 214, 372, 530 (blue circles).

ling operation also to satisfy such a requirement which in turn depends on the shear strength of the encountered soil layers.

For the piles of the considered subgroup the trend of the recorded parameters shows some partially random variability and some systematic change in the depth range between 15 m and 20 m. As an example, the recorded parameters for the descent phase of piles 214, 372 and 530 (location in Fig. 5), are plotted in Fig. 6. It can be seen that for piles 372 and 530 (Fig. 6b and 6c) the average drilling downwards velocity v together with the angular velocity n decreases below 13 m while the torque tends to increase. For pile 214 (Fig. 6a) the drilling technique clearly shows the other priority followed by the operators, i.e. maintaining constant the rotation velocity during the pile execution.

5. Failure loading tests on instrumented CFA piles

At the design stage two failure load tests (see location in Fig. 2) were carried out to obtain a reliable evaluation of the shaft ultimate capacity (S_u) and of the end bearing capacity (P_u) of the CFA piles.

The tests were carried out about 4 weeks after the pile installation was completed just to allow the concrete to develop the corresponding strength and stiffness.

The nominal geometry of the two piles was very similar, being both piles 0.8 m in diameter and approximately 24 m in embedded length. The pile 1 had a slightly longer top stretch out of the soil compared to the pile 2 (see Fig. 8). The high value of the load to be applied suggested to consider the option for an Osterberg's load cell test (Russo et al., 2003). Concern about the possibility to lower down the reinforcement cage with the load cell at the bottom in the fresh concrete, typical need for CFA piles, suggested to organise conventional load tests with a reaction system. The load tests consisted of a single cycle from zero up to the maximum test load, followed by unloading. To measure the separate mobilisations of the shaft resistance, S, and the end bearing capacity, P, the test piles were equipped with the removable tape extensometer developed at the LCPC in Paris (Bustamante and Jezequel, 1991; Russo, 2004).

The load-settlement curves (total load Q, shaft load S and base load P) and the axial load distributions along the pile shaft, obtained in the two load tests, are shown in Figs. 7 and 8. As shown by Russo (2013) even with the use of an heavy kentledge but for a pile characterized by a medium slenderness ratio, i.e. l/d = 30, the ultimate bearing capacity is not but negligibly affected by the test layout. On the other hand, the stiffness maybe significantly overestimated.

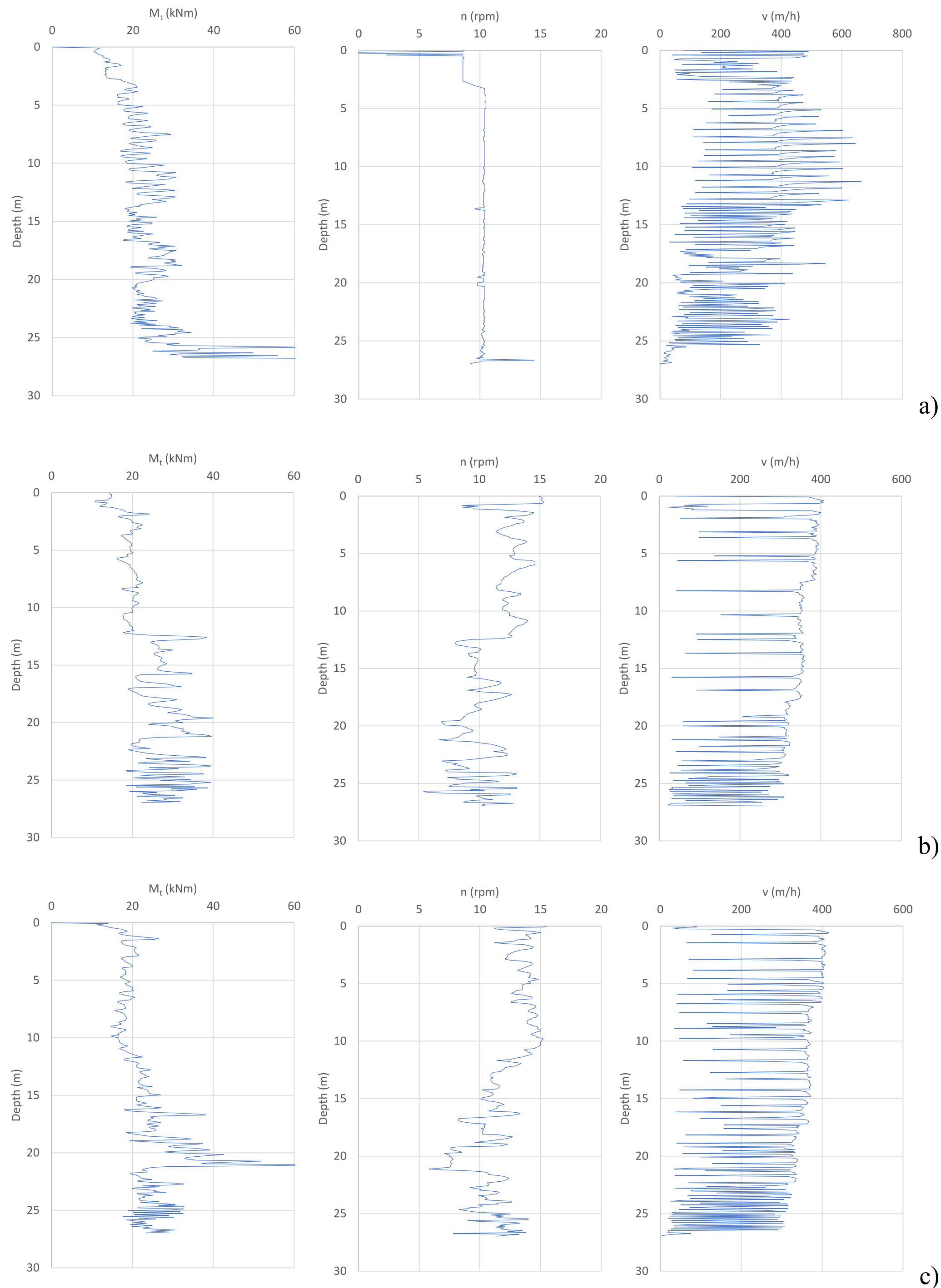

Fig. 6. Example of drilling parameters, measured for the realization of piles a) 214, b) 372 and c) 530, during the descent of the auger.

The load test on pile 1 was carried out up to a final state which was assumed in correspondence of a settlement of the order of 10 % of the nominal diameter of the pile d_N. The separate available trends of the shaft and the base mobilised capacity plotted in Fig. 7, show that, while the shaft capacity of the pile 1 after a peak slightly reduces to a residual value, the base load is still increasing. It is not surprising considering that for a replacement pile typically the end bearing is fully mobilised at settlements as large as 20–25 % of the pile diameter. The test on pile 2 was interrupted for safety reasons, being the maximum applied load (i.e. 5.26 MN) very close to the overall available reaction provided by weight of the kentledge system, at a much smaller value of the head settlement compared to the pile 1 ($\approx$3% d_N). On the other hand, this settlement is generally considered at least sufficient to mobilise the shaft resistance S. A confirmation of this may be obtained by comparing the latest two curves plotting the axial distri-

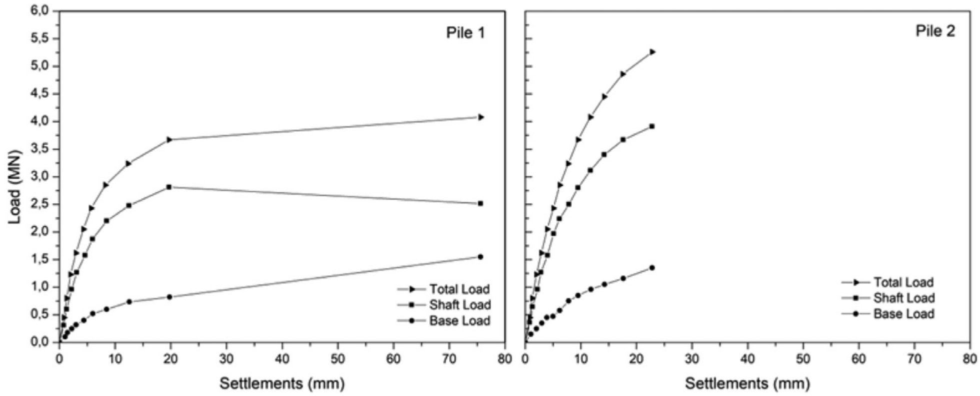

Fig. 7. Failure vertical load tests for piles 1 and 2.

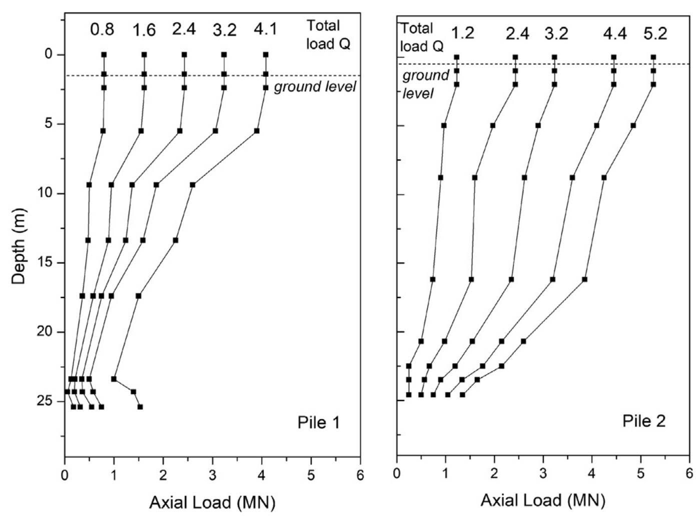

Fig. 8. Axial load distribution with depth at different Total Load Q for piles 1 and 2.

bution with the depth of the pile 2 which are nearly parallel.

In the Table 2 the main results of the two pilot loading tests are summarized. The maximum base load, P, is obviously deduced by the deepest points of the axial load distribution in Fig. 8 while the maximum shaft load, S, is deduced by the difference between the maximum total load, Q, and the maximum base load P.

The two pilot piles were expected to exhibit similar behaviors in terms of strength, as the available geotechnical investigations did not show any significant local variation at the location of pile 1 and 2 respectively. As a matter of fact, the tests show that pile 2 has both a larger stiffness and a larger bearing capacity when compared with pile 1. Furthermore, the separate results of the shaft and the base resistance made available using the removable extensometer clearly show that the overall shaft capacity of pile 2 is indeed larger than that obtained for pile 1. As could be suspected, the difference may be also due to a different installation procedure.

Observing the drilling parameters of the two piles (Fig. 9), in particular the penetration rate, it can be seen that pile 1 is characterized by an average ratio $v_{crit}/v \approx 1.55$ which is rather uniform with depth and determines a total net decompression effect on the surrounding soil; on the contrary, pile 2 has and average $v_{crit}/v \approx 0.95$ ratio which is rather uniform with depth along the shaft, apart from a moderate increase of the ratio close to the pile

Table 2
Failure tests on piles 1 and 2 (maximum values of the Total load, Base load and Shaft load) (*) not fully mobilised.

Pile	d (m)	L (m)	Total load, Q (MN)	Settlement, w_{max} (mm)	Base Load, P (MN)	Shaft load, S (MN)
1	0.8	24.0	4.08	75.6	1.55	2.81
2	0.8	24.1	5.26	22.8	1.46*	3.80

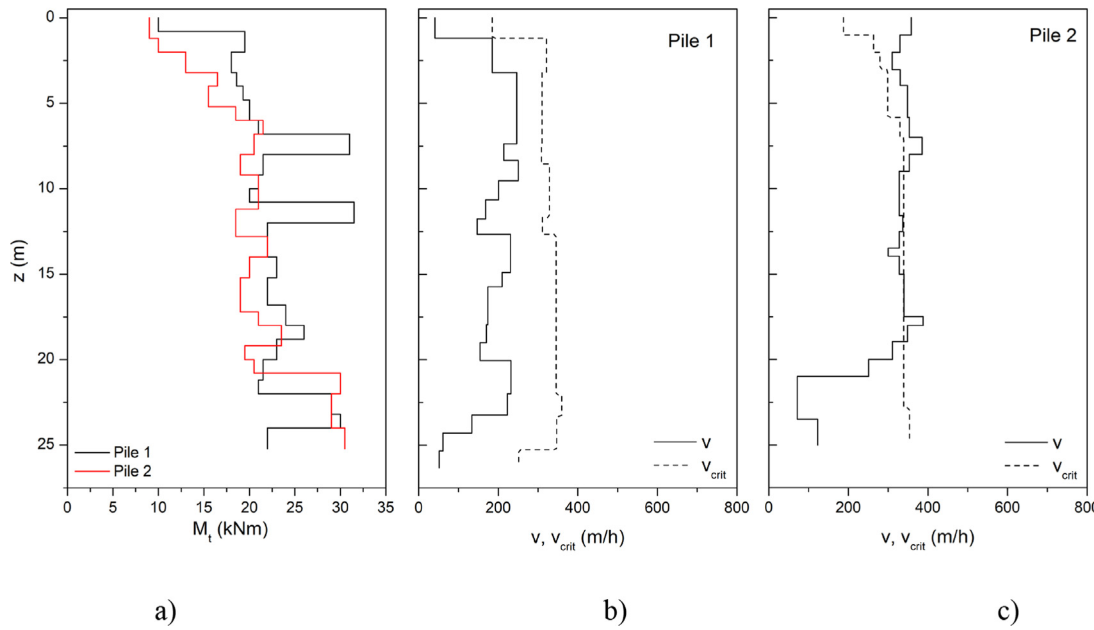

Fig. 9. Drilling parameter for piles 1 and 2: a) M_t for piles 1 and 2; b) penetration velocity, v and critical velocity, v_{crit} profiles for pile P1; c) drilling velocity v and critical velocity, v_{crit} for pile P2.

tip, resulting in a net average compression effect on the surrounding soil. In other words, even being both CFA piles with a theoretical expected intermediate behavior between a replacement and a displacement pile, pile 1, as confirmed by the measurements obtained via pile testing, is expected to exhibit lower shaft ultimate capacity compared to the pile 2. The ratio v_{crit}/v close to the pile tip is in the range of 4–5, very similar for both piles, and, also, the mobilized base load is very similar confirming the importance of the installation parameter v_{crit}/v on the pile performance.

6. Bearing capacity predictions of CFA piles by using CPT based methods and statistical correlations with drilling parameters

The two load tests carried out on similar CFA piles showed rather different behavior both in terms of stiffness and bearing capacity. Large differences were found mainly in the values of the ultimate shaft friction with the pile 2 showing a better performance. As explored in the previous section the larger penetration velocity v obtained by the drilling rig during the installation of the pile 2 may well qualitatively explain the observed differences.

On the other hand, in a more quantitative way, the bearing capacity of CFA piles in sandy soils is typically predicted at the design stage by empirical correlations with CPT results (Bustamante and Gianeselli, 1982; Viggiani, 1993; Reddy and Stuedlein, 2017). However, on one side the inherent variability of pyroclastic deposits is recognized to be generally quite large but, on the other side, the available CPTs profiles plotted in Fig. 4 do not show particular differences or trends as a function of the location inside the test site. As a matter of fact, in the previous section it was shown that the piling operator drilled the two piles in a rather different way. For this reason and to further explore the relationship between subsoil conditions, drilling parameters and pile performance the following procedure based on a statistical analysis of the available data is followed. As a first step, the drilling data are analyzed to propose correlations between the shear strength of the silty sand soil (usually measured via the cone resistance, q_c) and some of the drilling parameters measured during pile construction. After a trial-and-error procedure the focus is on the torque M_t, as it seems to be the most sensitive to variations in ground resistance. It is expected that for high values of q_c the applied torque increases and correspondingly for low values of the ground resistance the torque decreases (Gouvenot et al.,1990; Bustamante, 2003). In the next sections first a study of the statistical relation between torque M_t and cone resistance q_c has been carried out for all the piles of the subgroup where the drilling data were available. The obtained correlation has been than used to derive synthetic q_c profiles using the measured M_t profiles of the two load tested piles. Finally these CPT profiles have been used to calculate pile bearing capacity (Viggiani, 1993) and, mainly, the shaft resistance, which, as discussed in the previous section, is fully mobilised in both pile loading tests. All the statistical analyses have been carried out by R code (R Core Team 2013).

6.1. Statistical correlation between M_t and q_c

The correlation between CPT cone resistance q_c and the torque M_t is here analysed. All the available tests in the site area, i.e. 29 CPTs, are considered. From the trends shown in Fig. 10a, it can be seen that in the upper alluvial layer the

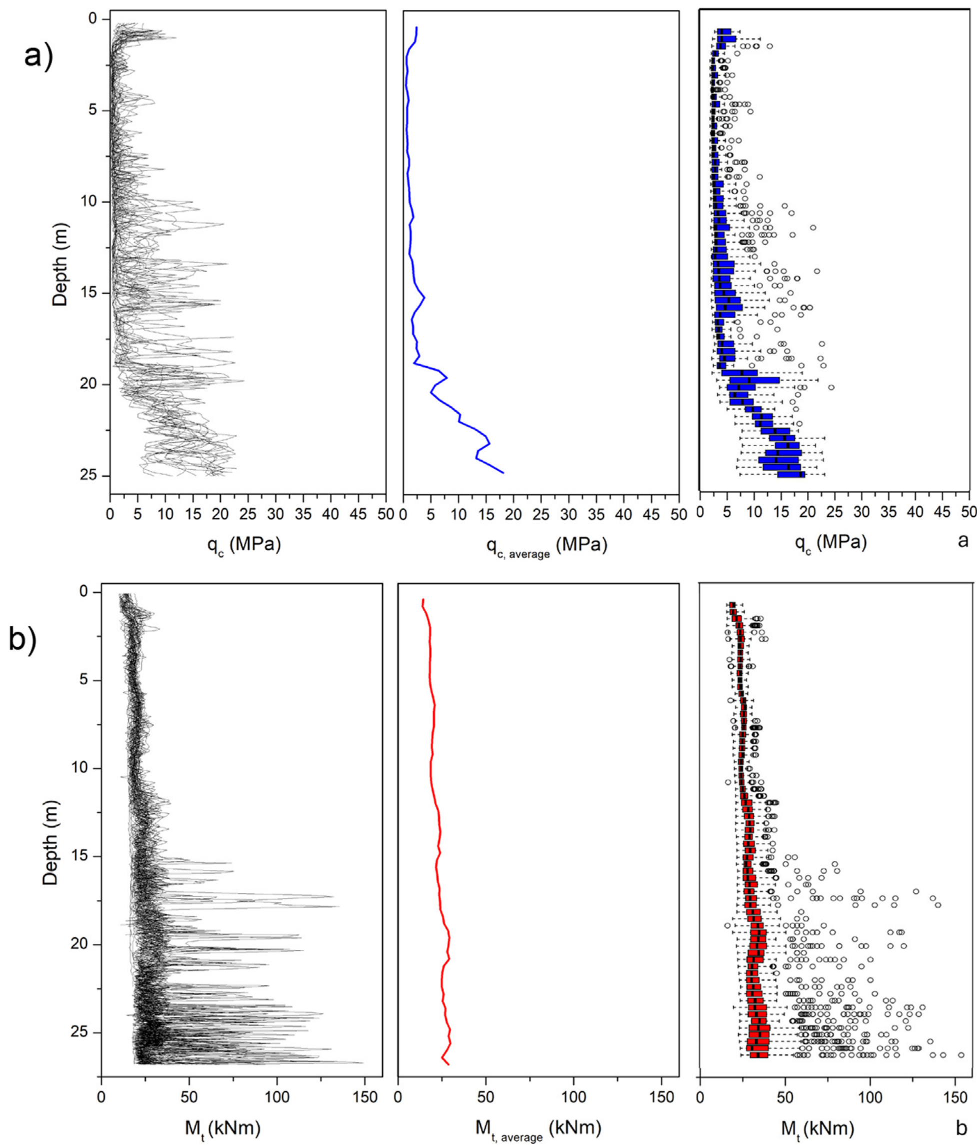

Fig. 10. Dataset, average trend and boxplot of a) tip resistance from CPT tests results b) torques from the selected CFA piles group.

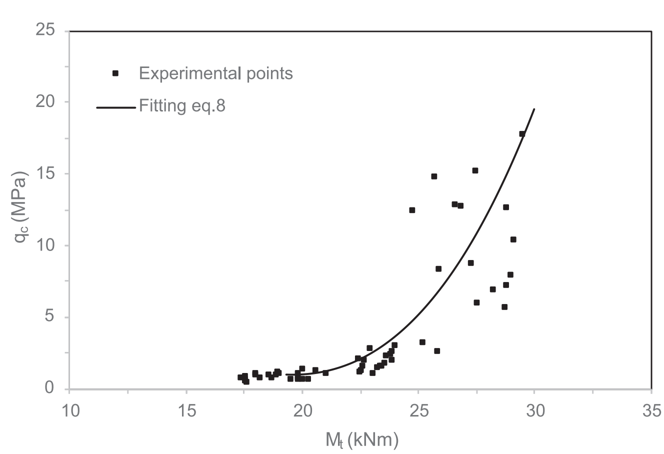

Fig. 11. Correlation between CPT cone resistance q_c and torque M_t at the same depth, z.

tip resistance is nearly constant with depth, whereas for the lower pyroclastic layer the variability of the tip values increases. Torques fully recorded for the 45 CFA piles of the selected subgroup show similar trend (Fig. 10b): in the alluvial formation they are characterised by a reduced variability, with a fairly constant average value with depth and maximum values never exceeding 50 kNm, while a more scattered distribution with larger and increasing with depth average values is shown in the pyroclastic formation. As shown by the boxplot in Fig. 10b, in this second layer the recorded torque M_t has maximum values as high as 150 kNm.

Using the average of the cone tip resistance and torque, the correlation between the two variables $q_c = (Mt)$ shown in Fig. 11 is characterised by a correlation coefficient $\rho = 0.719$ and is interpolated by a third-degree polynomial equation (interpolation coefficient $R^2 = 0.97$):

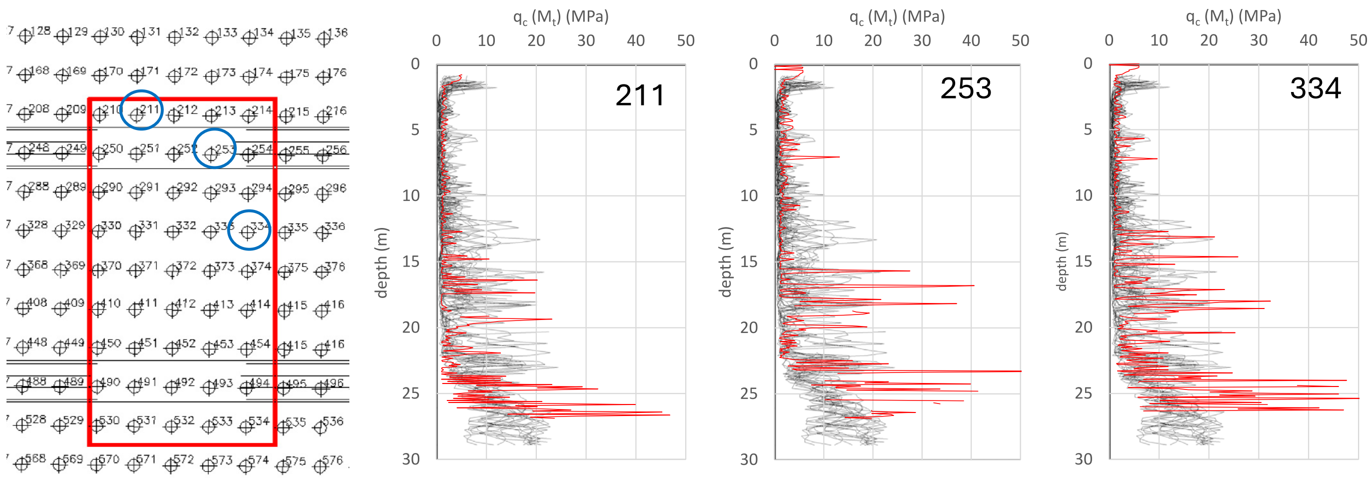

Fig. 12. Generated (in red) VS. measured (in black) CPT cone resistance q_c for piles 211, 253 and 344.

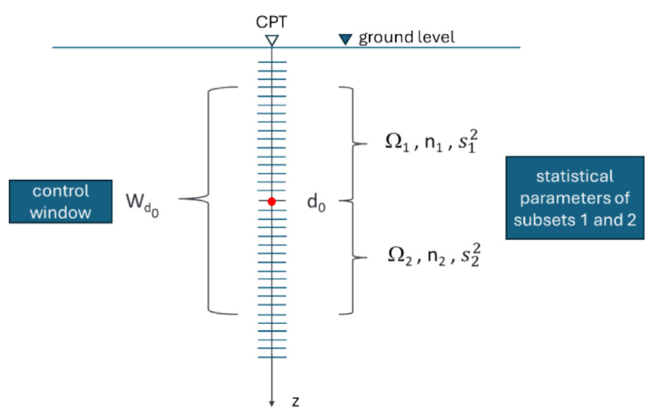

Fig. 13. Statistical method for detecting layers' change along CPT profile (. adapted from Spacagna et al. 2015)

$$q_c = 2.329M_t - 0.2299M_t^2 + 0.0058M_t^3 \tag{8}$$

As an example, the generated profiles of three of the selected piles (namely 211, 253 and 344), through the correlation proposed in Eq. (8), are compared with the overall population of CPTs in Fig. 12, highlighting the good correlation between the measured and the estimated q_c.

The stratigraphic features of the site (two main strata with quite different geotechnical properties) suggested to include the variability in depth of the soil parameters in the correlation between tip resistance and torque. For this purpose, to establish a more precise and objective depth of the layer's change in the proximity of the selected 45 subgroup piles, the available data related to the closest 3 CPT tests and 45 CFA piles (see Fig. 5) were used within the procedure proposed by Spacagna et al. (2015). Based on CPT test results, this method allows the identification of a change of layer along the vertical by means of a statistical test, originally proposed by Wickremesinghe & Campanella (1991), and supplemented with a geostatistical data selection criterion. The detection of the change of layer is based on the comparison of expected statistical characteristics of two independent sets of tip resistance values along the vertical, falling within a window of extent W_{d0} centred at point d_0 (Fig. 13). The T Student statistical test is repeated for the two sets for each subsequent position of the control window along the vertical. Statistically significant differences between the averages of two groups of values indicates a change of layer. Full description of the method is given in Appendix 1.

The tip resistances are correlated if they belong to the same soil layer (Wang et al. 2013; Ganju et al. 2017); a functional relationship between their values and position along the vertical defines a spatial structure (i.e., dependency of the measured value on its position along the vertical), which can be analysed using a variogram (Chiles & Delfiner, 1999) for evaluating the extent of the correlation between tip resistance values as a function of the mutual distance of the measurement points. In the present case, one-dimensional variogram was evaluated along each CPT vertical by considering the mutual distances between measurement points of tip resistance. The experimental variogram is well interpolated by a spherical variogram model, whose range (i.e., the maximum distance within

Table 3
Variographic analysis parameters and change of layer depths as deduced by the proposed procedure Spacagna et al. (2015).

CPT Test/Pile n.	Range	Sill	Nugget	Depth
	(m)	(MPa^2)	(MPa^2)	(m)
CPT-P2	1.6	5	7	14.2
CPT-E	2	4	1	14.4
CPT-B	1.6	4	5	14.6
250	0.8	60	50	16.9
251	2.56	50	30	15.9
414	1.12	60	60	14.6
453	1.6	37	75	15.0
491	1.44	12	16	15.1
492	1.12	12	8	15.9
494	1.2	15	25	14.9
531	1.12	15	10	14.7
533	1.28	20	20	15.2

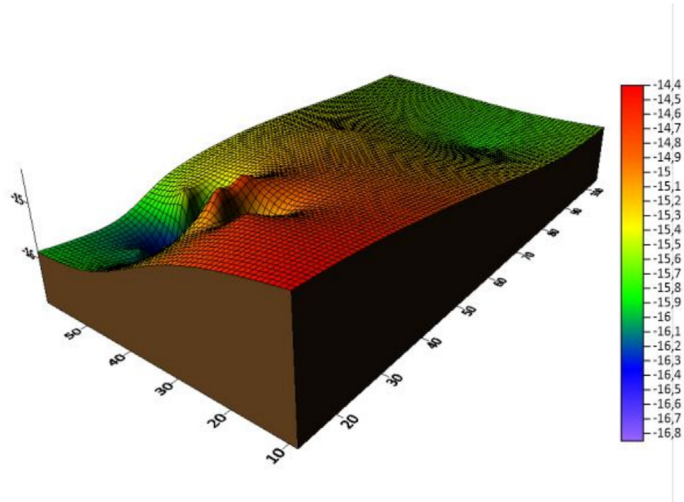

Fig. 14. 3D surface separation between upper alluvial and lower pyroclastic layers in the zone of the water treatment basin (coordinates and elevations in m).

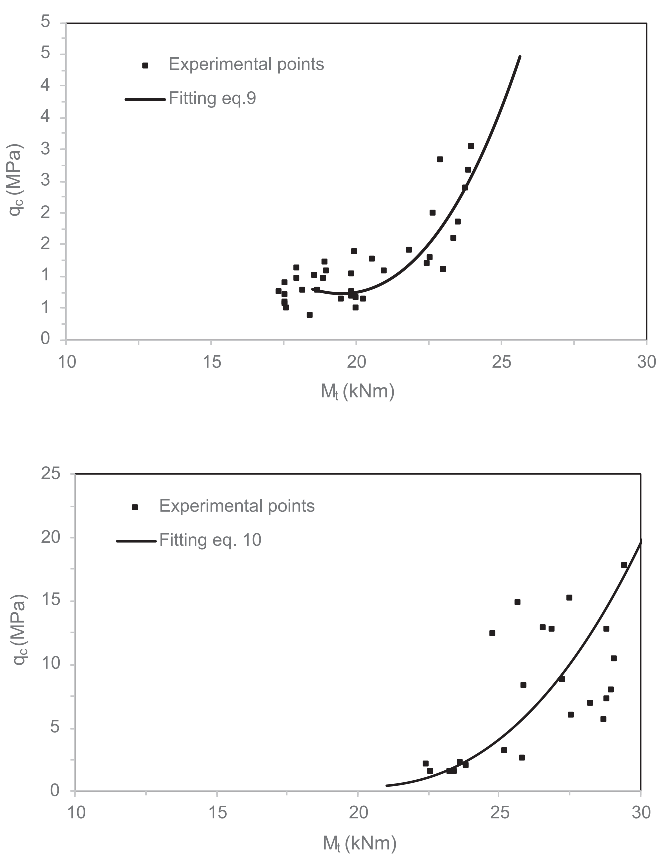

Fig. 15. Separate correlations between cone tip resistance and torques for alluvial layer, AL (upper) and pyroclastic layer, TG (lower).

which the values are correlated) allows the size of the control window for the statistical test to be dimensioned. The same procedure was implemented for both CPT tests and torques of the group of CFA piles selected for the study. The range values resulted within the interval 0.8 m ÷ 2.6 m. Assuming the width of the control window equal to the variogram range, the statistical test allowed identifying the change of layer along the examined vertical. Table 3 shows the parameters derived from the variographic analysis (range, sill and nugget) for the 3 CPT tests and for a sample of 10 out of the 45 piles together with the change of layer depths.

The local data obtained by the above procedure and the other information on the layer separation available at the boundary of the water treatment plant allowed to carry out a best fitting interpolation of the layer change depth by *kriging* method on the overall foundation area of the water treatment plant (Fig. 14). The surface between the two formations lies between 14.2 and 16.9 m b.g.l. and was assumed at an average depth of 16 m. On this statistically basis the cone tip resistance q_c and the torque M_t were divided into two subgroups (between the depths 0 m ~ 16 m and 16 m ~ 25 m b.g.l.). Two different correlations between tip resistance q_c and torque moments M_t were processed, the first for the upper alluvial deposits (correlation coefficient $\rho = 0.614$), the second for the lower pyroclastic layer (correlation coefficient $\rho = 0.302$). Fig. 15 shows the correlation data interpolated with the following third-degree polynomial relationships:

$$q_c = 1.558M_t - 0.154M_t^2 + 0.0039M_t^3 \quad (9)$$

$$q_c = 2.838M_t - 0.277M_t^2 + 0.0068M_t^3 \quad (10)$$

where the Eq. (9) is referred to the upper layer (Eq. (9)), interpolation coefficient $R^2 = 0.937$) and the Eq. (10) is referred to the lower layer (Eq. (10), interpolation coefficient $R^2 = 0.979$).

6.2. Model validation: Calculation of the pile ultimate capacity

In the previous section a statistical analysis of the available torque profiles for a significant group of piles has been carried out showing a close correlation with the tip resistance of CPT profiles. Furthermore, the procedure by Spacagna et al. (2015) allowed to more precisely determine the depth of separation between the top alluvial layer and the bottom pyroclastic layer and as a consequence two different correlations for the two layers were proposed (i.e. Eqs. (9) and (10)). In this section the shaft resistance as measured for the two load tested piles is compared with the one theoretically calculated using classical CPT based methods. The novelty of the proposed approach consists in adopting for such calculation information provided by the recorded drilling parameters. To this aim the following procedure has been adopted. The ultimate shaft capacity, S_u, of the two piles P1 and P2 is computed starting from synthetic CPT results obtained via the drilling parameter M_t, using the q_c (M_t) relations (see Figs. 11 and 15).

The procedure for the calculation of the bearing capacity has been applied twice for each pile using both correlations analysed in the previous section (i.e., Eq. (8), derived for a unique soil layer, and Eqs. (9) and (10), based on the separation in two distinct layers).

Once a q_c profile is available the bearing capacity of CFA piles can be computed according to different empirical methods (Mihálik et al., 2023; Brown et al., 2007; Gavin et al., 2021). However the method proposed by Viggiani (1993) for designing CFA piles in pyroclastic soils was selected for two main reasons: first, the overall database of the method could be handled by the authors in order to apply it in a more conscious way and, second

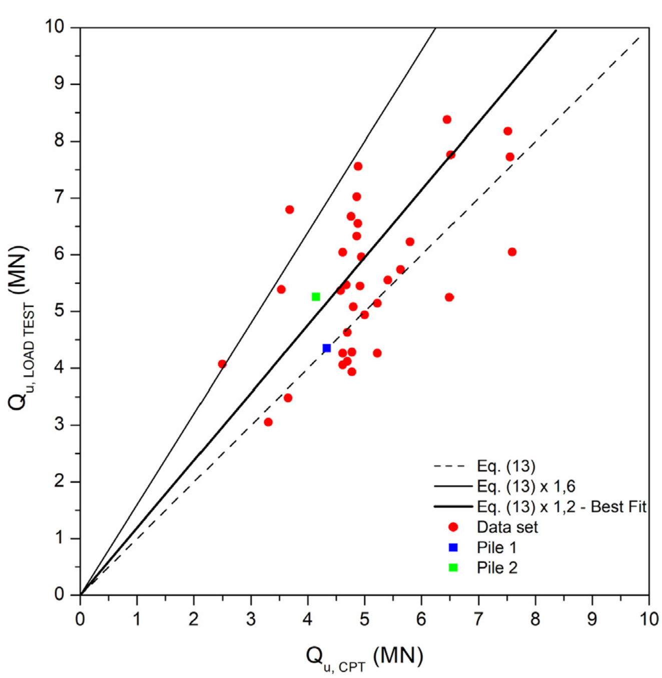

Fig. 16. Comparison between experimental data ($Q_{u,\ load\ test}$) and computed ultimate capacity $Q_{u,CPT}$: data set by Viggiani (1993) and the additional points representative of the behaviour of the two load tested piles Pile 1 and Pile 2.

and more important, both the pile technology and the type of the subsoil were similar to those of the two tested piles.

Viggiani (1993) proposed that CFA bearing capacity could be obtained by calculating the base ultimate capacity, q_p, as the average value of q_c computed between the depth $z = L\text{-}4D$ and $z = L + 4D$ (Meyerhof, 1976):

$$q_p = \bar{q}_c\,(z = L - 4D, z = L + 4D) \tag{11}$$

but with a cutoff on the measured q_c at 8 MPa.

The unit ultimate local shaft capacity was proposed as (Viggiani, 1993):

$$s(z) = \alpha \cdot q_c(z) \tag{12}$$

with α obtained by the following equation as a function of the $q_c(z)$:

$$\alpha = \frac{6.6 + 0.32 q_c(z)(MPa)}{300 + 60 q_c(z)(MPa)} \tag{13}$$

These values were obtained by Viggiani (1993) based on a dataset (red full dots in Fig. 16) of available load tests and produced the agreement as reported in Fig. 16. It can be clearly seen by the Fig. 16 and commented here that the equations proposed by Viggiani (1993) are surely conservative being most of the experimental points, i.e. the red full dots, located in the upper quadrant of the cartesian plane with the y-axis representing the measured bearing capacity $Q_{u,\ LOAD\ TEST}$ and the x-axis represented the bearing capacity $Q_{u,\ CPT}$ computed using (11), (12) and (13).

Then the above method was applied for each of the two piles P1 and P2 twice using two synthetic $q_c(M_t(z))$ profiles and obtaining the results summarized in Table 4.

The second column of the Table 4 is considered by a statistical point of view the most correct and the agreement in the case of pile n.1 is excellent while in the first column a significant overestimate is produced by the equation (8) which was obtained neglecting the difference between the two soil layers. It is worthy reminding that end bearing during the pile test is quite evidently not fully mobilised and as such the comparison here is limited to the shaft friction. For the pile n.2 even considering the second column of the Table 4 the agreement is not that satisfactory the ratio between the measured and the calculated value being about 1.40.

However, it was shown that the CPT method (Viggiani, 1993) adopted to calculate the shaft capacity was empirically based and inspired to a conservative approach. Thus it is not surprising that for the pile P1, which is characterized along the overall shaft by drilling speed profiles typical of a replacement pile with a significant net decompression effect, the agreement between a conservative design approach for CFA piles and the measured performance is excellent. For the same reason it is again not surprising that for a very *well-done* CFA pile, i.e. the pile P2, which is characterized by a more virtuous drilling speed profiles, characterized by a significant net compression effect on the surrounding soil, the application of the design method is producing a shaft capacity much smaller than the measured

Table 4
Shaft ultimate capacity from $q_c(M_t(z))$ correlations compared with shaft ultimate capacity from load tests.

	S_u from $\alpha \cdot q_c(M_t)$ Eq.(8), Eq.(13)	S_u from $\alpha \cdot q_c(M_t)$ Eq.(9), Eq. (10), Eq.(13)	S_u from load test
Pile n.1	3.44 MN	2.76 MN	2.80 MN
Pile n.2	2.98 MN	2.68 MN	3.80 MN

value. As shown in Fig. 16 (modified after Viggiani, 1993) simply removing the conservatism of the design approach proposed by Viggiani and adopting an average value (i.e. the best fit line) on the same experimental dataset the pile total ultimate capacity should be calculated with Eqs. (12) and (13) multiplied by a factor of 1.2. This line is not only the line that best fit the old data set by Viggiani but is also very close to the point representative of the pile P2 presented in the paper. In the same direction it is worth mentioning that the straight continuous line representing the upper bound of the overall experimental dataset nearly correspond to a multiplication factor as high as 1.60 well above the experimentally determined 1.40.

7. Conclusions

This paper presents two pilot load tests conducted on instrumented CFA piles, with detailed records of drilling parameters. These pilot tests were planned during the design stage of a large rectangular water treatment plant, which was founded on a large group of CFA piles. The study shows that an important source of the variations in pile performance can be attributed to differences in drilling parameters, particularly in penetration speed profiles. Soil investigations primarily relied on CPT profiles. For a selected subgroup of piles, installation parameters such as rotation velocity (n, in rpm), penetration velocity (v), and applied torque (M_t) with depth were carefully recorded. Initially, a statistical method was applied to the available CPT profiles, successfully identifying two main soil layers with distinct behaviors. The depth of the separation obtained through this analysis corresponded well and more accurately specified the qualitative geological information described in Section 2.

Further statistical analysis revealed a robust correlation between the cone resistance (qc(z)) from CPT tests and the torque ($M_t(z)$) required during auger installation. Two correlation models were developed, with the best fit observed when accounting for the two-layer separation. The bearing capacities of CFA piles and mainly the pile shaft ultimate capacity, measured during load tests, were used as benchmarks to validate calculations performed using an empirically derived CPT-based method (Viggiani, 1993). These calculations utilized "synthetic" CPT profiles generated from the torque values (M_t) recorded during pile installation. The application of the empirical method demonstrated excellent agreement, as discussed in Section 6.2, with the measured pile performance, confirming that drilling torques can serve as a reliable alternative to CPT profiles.

The influence of drilling speed (v) on observed pile performance was also highlighted. Practically, these findings suggest that it is possible to verify or recalculate the expected performance of installed piles based on the recorded torque values. Additionally, the variability in pile group behavior can be reassessed using the recorded drilling parameters, allowing for potential design modifications if necessary.

Lastly, experimental results from the two instrumented test piles confirm that the behavior of CFA piles lies between that of bored and driven piles, with performance strongly influenced by installation procedures and details. Beyond the penetration stage, factors such as extraction procedures and the volume of concrete supplied during extraction may also significantly affect pile performance. It may be foreseen that a systematic monitoring of installation parameters, both in the penetration and extraction stages, can provide useful data for a direct evaluation of the bearing capacity of CFA piles.

CRediT authorship contribution statement

Gianpiero Russo: Writing – review & editing, Writing – original draft, Visualization, Validation, Supervision, Methodology, Formal analysis, Data curation, Conceptualization. **Ilaria Esposito:** Writing – original draft, Visualization, Methodology, Data curation. **Massimo Ramondini:** Visualization, Investigation, Data curation. **Alessia Vecchietti:** Software. **Giacomo Russo:** Writing – review & editing, Writing – original draft, Visualization, Validation, Software, Methodology, Formal analysis, Data curation, Conceptualization.

Acknowledgements

This study was partially funded by the European Union - NextGenerationEU_, in the framework of the_GRINS - Growing Resilient, INclusive and Sustainable_project (MUR: GRINS PE00000018 – CUP E63C22002140007). The views and opinions expressed are solely those of the authors and do not necessarily reflect those of the European Union, nor can the European Union be held responsible for them. The Authors thank dr. Maria Vicario and dr. Sara Sansone for their valuable support in data processing and statistical analyses.

Appendix 1. Stratigraphical interpretation of CPT and M_t profiles by statistical approach

The method applied is based on the Student T-test aimed at the verification of equality of the means, according to the procedure shown in Fig. 11. With reference to the tip resistance q_c of CPT tests and torque M_t profiles along the vertical axis, a window W_{d0} is centered around point d_0. The depth where point d_0 is located has been hypothesized as the transition between two different lithological layers. The opening of the window W_{d0} includes two subsets of data, namely Ω_1 and Ω_2, with size respectively equal to n_1 and n_2, average $\bar{Q}_1$ and $\bar{Q}_2$ and variance σ_1^2 and σ_2^2.

The value of the Student parameter T is defined in the Eq. (A1), as suggested by Webster and Beckett (1968):

$$T = \frac{\bar{Q}_1 - \bar{Q}_2}{\gamma_w}\sqrt{\frac{n_1 n_2}{n_1 + n_2}} \tag{A1}$$

where:

$$\gamma_w = \frac{n_1}{n_1 + n_2 - 1}\sigma_1^2 + \frac{n_2}{n_1 + n_2 - 1}\sigma_2^2 \tag{A2}$$

$$\sigma_1^2 = \frac{1}{(n_1 - 1)}\sum_{i=1}^{n_1}\left(Q_i - \bar{Q}_1\right)^2 \tag{A3}$$

$$\sigma_2^2 = \frac{1}{(n_2 - 1)}\sum_{i=1}^{n_2}\left(Q_i - \bar{Q}_2\right)^2 \tag{A4}$$

The intraclass correlation coefficient ρ_I is calculated using Eq. (A5):

$$\rho_I = \frac{\gamma_b^2}{\gamma_b^2 + \gamma_w^2} \tag{A5}$$

The variance between class γ_b^2 is defined by the Eq. (A6):

$$\gamma_b^2 = \frac{1}{n_1 + n_2 - 1}\sum_{i=1}^{n_1+n_2}\left(Q_i - \bar{Q}\right)^2 \tag{A6}$$

where $\bar{Q}$ is the average of the data Q_i belonging to the window w_{d0}, with $i = 1,2, \ldots, (n_1 + n_2)$.

The window W_{d0} should contain possibly only one change of subsoil layer, and therefore its amplitude cannot be chosen arbitrarily. If W_{d0} was too wide, more of one change of layer could be included in the selected window; on the opposite, a small amplitude of the window W_{d0} does not provide enough data for a reliable statistical inference. Webster (1973) suggested a size of the window equal to two-thirds of the expected distance between different layers of the subsoil, while Wickremesinghe and Campanella (1991) considered the 2/3 of the spatial autocorrelation of the data as the reference amplitude of the window. In this paper, the width of the window was selected by a geostatistical approach (Spacagna et al. 2015), as described in chapter 6.1.

The Student T and intraclass coefficient ρ_I are calculated for each couple of subsets obtained by the translation of the window W_{d0} along the vertical axis centered in each point d_0. Two new profiles are then available, namely the T and ρ_I profiles with depth. Along with the new two profiles, higher values correspond to possible changes of the lithological strata. The critical value of the parameter T is calculated as follows:

$$T_c = \mu_T \pm 1.65\sigma_T \tag{A7}$$

where μ_T and σ_T are respectively the mean and standard deviation of the normal distribution describing the variable T. The critical value of the intraclass correlation coefficient, ρ_{Ic}, was also calculated using the relationship proposed by Herzagy et al. (1996):

$$\rho_{Ic} = \mu_{\rho I} \pm 1.65\ \sigma_{\rho I} \tag{A8}$$

where $\mu_{\rho I}$ and $\sigma_{\rho I}$ are respectively the mean and standard deviation of the normal distribution describing the variable ρ_I.

As an example, in Fig. A1 the T and ρ_I profiles based on CPT-P2 profile are reported with the critical values of the statistical parameters individuating the possible change of layer.

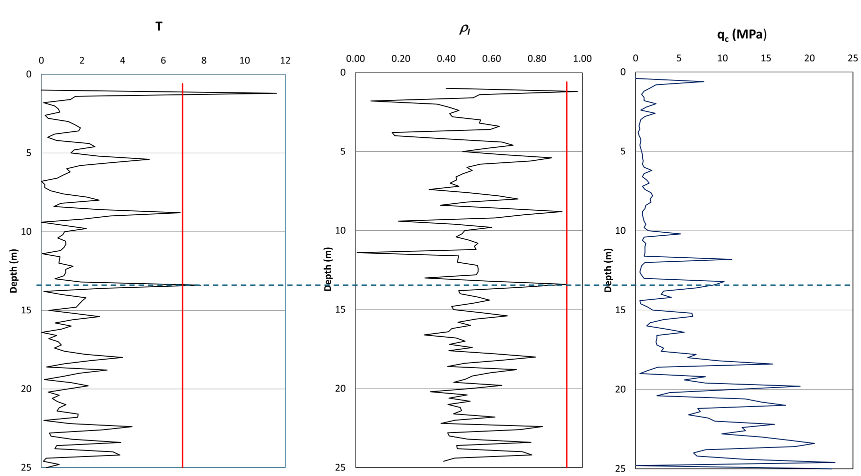

Fig. A1 Stratigraphical interpretation of CPT-P2 profile by means of statistical approach.

References

Brown, D.A, Dapp, S.E., Thompson, R.W., Lazarte, C.A., 2007. Design and construction of continuous flight auger piles final. Research Report FHWA-HIF-07-03.

Bustamante, M. 2003. Auger and Bored pile monitoring and testing. Theme Lecture, Proc., 4th Int. Symp. on Deep Foundations on Bored and Auger Piles, Van Impe ed., Ghent, Balkema, Rotterdam, 27-43.

Bustamante, M. Gianeselli, L. 1982. Pile bearing capacity prediction by means of static penetrometer CPT. Ed. Balkema. Proc. of 2nd Eur. Symp. On Penetration testing, Esopt II, Amsterdam.

Bustamante, M., Jezequel, J.F. 1991. "La mesure des deformations a l'aide des estensiometeres amovible." LCPC Methode d'essai n°34 LEPC, Paris.

Chen, Y., Deng, A., Lu, F., Sun, H., 2020. Failure mechanism and bearing capacity of vertically loaded pile with partially-screwed shaft: Experiment and simulations. Comput. Geotech. 118. https://doi.org/10.1016/j.compgeo.2019.103337.

Chiles, J., Delfiner, P., 1999. Geostatistics: modeling spatial uncertainty. John Wiley and Sons, New York.

Di Maio, R., Fabbrocino, S., Forte, G., Piegari, E., 2014. A three-dimensional hydrogeological-geophysical model of a multi-layered aquifer in the coastal alluvial plain of Sarno River (southern Italy). Hydrgeol. J. 22 (3), 691.

Doan, L.V., Lehane, B.M., 2021. CPT-based design method for axial capacities of drilled shafts and auger cast-in-place piles. J. Geotech. Geoenviron. Eng. 147 (8). https://doi.org/10.1061/(ASCE)GT.1943-5606.0002542.

Eslami, A., Fellenius, B.H., 1997. Pile capacity by direct CPT and CPTu methods applied to 102 case histories. Can. Geotech. J. 34 (6), 886–904. https://doi.org/10.1139/T97-056.

Ganju, E., Prezzi, M., Salgado, R., 2017. Algorithm for generation of stratigraphic profiles using cone penetration test data. Comput. Geotech. 90 (2017), 73–84.

Gavin, K., Kovacevic, M.S., Igoe, D., 2021. A review of CPT based axial pile design in the Netherlands. Underground Space 6 (1), 85–99. https://doi.org/10.1016/J.UNDSP.2019.09.004.

Gouvenot, D., Hamelin, J.P., La Fonta, J.G., 1990. L'electronique et l'informatique au service des travaux de foundation. Mem. Soc. Geol. de France, ns. 157, 1-11.

Han, F., Salgado, R., Prezzi, M., Lim, J., 2017. Shaft and base resistance of non-displacement piles in sand. Comput. Geotech. 83, 184–197. https://doi.org/10.1016/j.compgeo.2016.11.006.

Heidarie Golafzani, S., Eslami, A., Jamshidi Chenari, R., 2020. Probabilistic Assessment of Model Uncertainty for Prediction of Pile Foundation Bearing Capacity; Static Analysis, SPT and CPT-Based Methods. Geotech. Geol. Eng. 38 (5), 5023–5041. https://doi.org/10.1007/S10706-020-01346-X.

Herzagy, Y., Mayne, P., Rouhani, S., 1996. Geostatistical assessment of spatial variability in piezocone tests. Uncertainty in geologic environment: from theory to practice (GSP 58), ASCE, New York, 254–268.

Leetsaar, L., Korkiala-Tanttu, L., Kurnitski, J., 2023. CPT, CPTu and DCPT Methods for Predicting the Ultimate Bearing Capacity of Cast In Situ Displacement Piles in Silty Soils. Geotech. Geol. Eng. 41 (2), 631–652. https://doi.org/10.1007/S10706-022-02292-6.

Mandolini A., Ramondini, M., Russo, G., Viggiani, C., 2002. Full scale loading tests on instrumented CFA piles. In Deep Foundations 2002: An International Perspective on Theory, Design, Construction, and Performance (pp. 1088-1097).

Massarsch, K.R., Tancre, E., Brieke, W., 1988. "Displacement auger piles with compacted base". Proc., 1st Int. Symp. on Deep Foundations on Bored and Auger Piles, Van Impe ed., Ghent, Balkema, Rotterdam, 333-342.

Meyerhof, G.G., 1976. Bearing capacity and settlement of pile foundations. Journal of the Geotechnical Engineering Division 102 (3), 197–228.

Mihálik, J., Gago, F., Vlček, J., Drusa, M., 2023. Evaluation of methods based on CPTu testing for prediction of the bearing capacity of CFA piles. Applied Sciences (Switzerland) 13 (5). https://doi.org/10.3390/APP13052931.

Niazi, F.S., Mayne, P.W., 2016. CPTu-based enhanced UniCone method for pile capacity. Eng. Geol. 212, 21–34. https://doi.org/10.1016/j.enggeo.2016.07.010.

Reddy, S. C., A. W. Stuedlein., 2017. "Ultimate limit state reliability-based design of augered cast-in-place piles considering lower-bound capacities." Can. Geotech. J., 54 (12): 1693–1703. Canadian Science Publishing. doi: 10.1139/CGJ-2016-0145.

Russo, G., 2013. Experimental investigations and analysis on different pile load testing procedures. Acta Geotech. https://doi.org/10.1007/s11440-012-0177-4.

Russo, G., 2004. Full-scale load tests on instrumented micropiles. Proc. Inst. Civ. Eng. Geotech. Eng. doi: 10.1680/geng.2004.157.3.127.

Russo, G., Recinto, B., Viggiani, C., de Sacntis, L., 2003. A contribution to the analysis of Osterberg's cell load test Proc., 4th Int. Symp. on Deep Foundations on Bored and Auger Piles, BAP IV, Van Impe ed., Ghent, Balkema, Rotterdam, 331-338 ISBN 90-77017-76-3.

Spacagna R.L., de Fouquet C., Russo G., 2015. Interpretation of CPTU test with statistical and geostatistical methods. Geotechnical Safety and Risk V, T. Schweckendiek et al. (Eds.), IOS Press, Pages 910 - 916. 10.3233/978-1-61499-580-7-910.

Van Impe, W.F., Peiffer, H., 1997. "Influence of screw pile installation on the stress state in the soil." Proc., ERTC3 Seminar on Design of axially loaded piles – European practice, De Cock & Legrand eds., Balkema, Rotterdam, 3–19.

Van Weele, A.F., 1988. "Cast in situ piles. Installation methods, soil disturbance and resulting pile be-haviour." Proc., 1st Int. Symp. on Deep Foundations on Bored and Auger Piles, Van Impe ed. Ghent, Bal-kema, Rotterdam, 219-226.

Viggiani, C., 1993. "Further experiences with auger piles in Naples area." Proc., 2nd Int. Symp. on Deep Foundations on Bored and Auger Piles, Van Impe ed. Ghent, Balkema, Rotterdam, 445-455.

Wang, Y., Huang, K., Cao, Z., 2013. Probabilistic identification of underground soil stratification using cone penetration tests. Can. Geotech. J. 50, 766–776. https://doi.org/10.1139/cgj-2013-0004.

Webster, R., 1973. Automatic soil Boundary Location from Transect Data. Journal of Mathematical Geology 5, 27–37.

Wickremesinghe, D., Campanella, R., 1991. Statistical Methods of Soil Layer Boundary Location Using the Cone Penetration Test, Proc., 6 th Int. Conf. on application of Statistics and Probability in Civil Engineering, CERRA-ICASP6, 636–644.

Webster, R., Beckett, P.H.T., 1968. Quality and usefulness of soil maps. Nature 219 (5155), 680–682.

Xu, X., Lehane, B.M., 2008. Pile and penetrometer end bearing resistance in two-layered soil profiles. Geotechnique 58 (3), 187–197. https://doi.org/10.1680/GEOT.2008.58.3.187.

Zelada, G.A., Stephenson, R.W., 2000. Design Methods for Auger CIP Piles in Compression. Proceedings of Sessions of Geo-Denver 2000 - New Technological and Design Developments in Deep Foundations, GSP 100, 288, 418–432. doi: 10.1061/40511(288)30.